Journal of Clinical Imaging Science

Editor-in-Chief: Vikram S. Dogra, MD
Department of Imaging Sciences, University of Rochester Medical Center, Rochester, USA

OPEN ACCESS
HTML format

For entire Editorial Board visit : www.clinicalimagingscience.org/editorialboard.asp

www.clinicalimagingscience.org

PICTORIAL ESSAY

Shoulder Ultrasonography: Performance and Common Findings

Diana Gaitini

Department of Medical Imaging, Unit of Ultrasound, Rambam Health Care Center and Bruce Rappaport Faculty of Medicine, Israel Institute of Technology, Haifa, Israel

Address for correspondence:
Prof. Diana Gaitini, Clinical Assistant Professor, Director, Ultrasound Unit, Senior Radiologist, Department of Medical Imaging, Rambam Medical Center, Technion-Israel Institute of Technology, Ha'aliya - 8, POB - 9602, Haifa, 31096 - Israel.
E-mail: d_gaitini@rambam.health.gov.il

Received : 02-02-2012
Accepted : 07-05-2012
Published : 28-07-2012

ABSTRACT

Ultrasound (US) of the shoulder is the most commonly requested examination in musculoskeletal US diagnosis. Sports injuries and degenerative and inflammatory processes are the main sources of shoulder pain and functional limitations. Because of its availability, low cost, dynamic examination process, absence of radiation exposure, and ease of patient compliance, US is the preferred mode for shoulder imaging over other, more sophisticated, and expensive methods. Operator dependence is the main disadvantage of US examinations. Use of high range equipment with high resolution transducers, adhering to a strict examination protocol, good knowledge of normal anatomy and pathological processes and an awareness of common pitfalls are essential for the optimal performance and interpretation of shoulder US. This article addresses examination techniques, the normal sonographic appearance of tendons, bursae and joints, and the main pathological conditions found in shoulder ultrasonography.

Key words: Anatomy, musculoskeletal imaging, shoulder, ultrasonography

INTRODUCTION

Imaging of the shoulder is a common investigation requested in patients presenting with shoulder pain and functional disabilities. A wide variety of etiologies, from rotator cuff pathologies to calcifying tendinosis, synovitis, acromioclavicular arthritis, and cervical radiculopathy may lead to similar symptoms. Shoulder arthrography and magnetic resonance imaging have been the imaging modalities commonly used to distinguish among these conditions.[1-2] The development of musculoskeletal ultrasonography, based on advanced ultrasound (US) capabilities, has enabled this technique to be included as a primary imaging investigation among the battery of available diagnostic tests.[3]

Knowledge of optimal techniques, normal anatomy, dynamic maneuvers, and pathological conditions is essential for correct US imaging and interpretation.[4] Shoulder US should strictly adhere to the imaging protocol.[5] Comparison between the damaged and the contralateral sides may aid in reaching diagnostic conclusions.

Access this article online	
Quick Response Code:	Website: www.clinicalimagingscience.org
	DOI: 10.4103/2156-7514.99146

This article may be cited as:
Gaitini D. Shoulder Ultrasonography: Performance and Common Findings. J Clin Imaging Sci 2012;2:38.
Available FREE in open access from: http://www.clinicalimagingscience.org/text.asp?2012/2/1/38/99146

This pictorial essay aims to illustrate the technical performance, normal anatomy, and main pathologies related to the rotator cuff and beyond, as well as pitfalls in the US examination of the shoulder.

Performance protocol and normal anatomy

Modern US systems, offering high resolution multifrequency linear array transducers ranging from 4 to 7, 3 to 9, 5 to 12 and 5 to 17 MHz, and color Doppler capabilities, enable optimal definition of anatomical structures. Bone surface, tendons, bursae, ligaments, and muscles can be clearly demonstrated. A checklist protocol is proposed for a systematic shoulder US examination [Table 1].

Shoulder ultrasound starts by examining the bicipital groove (BG) and long head of the biceps brachii tendon. The patient is seated facing the operator in a neutral position, his/her hand placed palm up on the thigh. A short axis image is performed by positioning the transducer over the proximal humeral metaphysis perpendicular to the humerus. The long axis image of the tendon is obtained by rotating the transducer to a position parallel to the humeral shaft [Figure 1]. Then, the subscapularis tendon is examined. Patient's arm is fixed on the flank and the forearm abducted in external rotation. Long and short axis views of the tendon are performed [Figure 2]. The infraspinatous and teres minor tendons are examined from a posterior view of the shoulder The patient is rotated 90°, his/her hand placed over the opposite shoulder and the transducer oriented in the axial plane over the head of the humerus [Figure 3]. The glenohumeral joint and the spinoglenoid notch are also examined on a posterior view of the shoulder. The transducer is now moved medially and caudally in the transverse plane until the posterior margin of the glenohumeral joint is seen and then, further medially to show the spinoglenoid notch [Figure 4]. The supraspinatous tendon is scanned on an anterior view of the shoulder. The patient is seated facing the operator. Patient's arm is placed in a posterior position, the dorsal hand on the opposite iliac wing or the palmar hand on the ipsilateral iliac wing. Long and short axis views of the supraspinatous tendon are obtained. Scanning of the rotator cuff is then performed during dynamic

Table 1: Proposed checklist for Shoulder US examination

Bicipital groove and long head of the biceps brachialis tendon [Figure 1]
Subscapularis tendon [Figure 2]
Infraspinatous and teres minor tendons [Figure 3]
Glenohumeral joint and spinoglenoid notch [Figure 4]
Supraspinatous tendon; dynamic maneveurs [Figure 5]
Acromioclavicular joint [Figure 6]

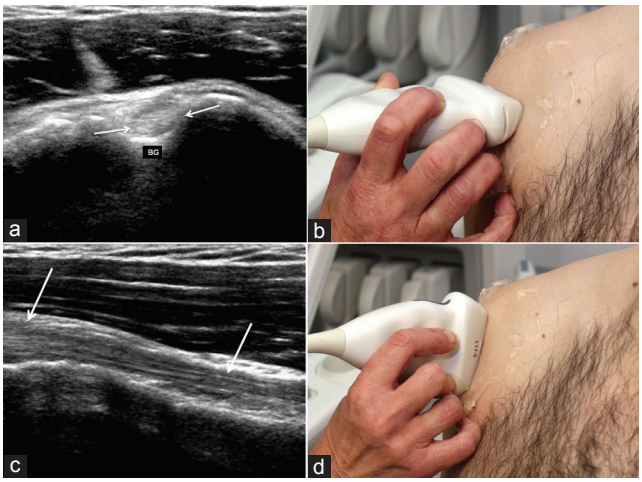

Figure 1: Bicipital groove (BG) and long head of the biceps brachii tendon. (a) Short axis image. The normal biceps tendon is a rounded echogenic structure (arrows) surrounded by a thin sonolucent area representing a small amount of fluid in the synovial sheath; the echogenic transverse ligament is seen superficial to the tendon. The bicipital groove (BG) is identified at the anterior aspect of the humeral head as a concave echogenic line. (b) The position of the transducer on the bicipital groove of the humerus. (c) Long axis image shows the fine fibrillar structure of the biceps tendon (arrows). (d) The position of the transducer along the humeral shaft to view the long head of the biceps tendon.

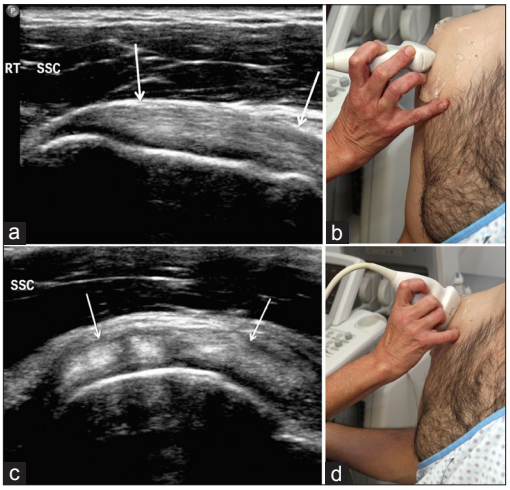

Figure 2: Subscapularis tendon. (a) Long axis view of the tendon. A fibrillar pattern is seen along the tendon (arrows), which inserts into the lesser tuberosity (LS). (b) The transducer is placed in an axial plane for a long view of the tendon. (c) Short axis view of the tendon shows a series of hyperechoic fibers and hypoechoic clefts, due to interposed muscle fibers among the tendon fibers (arrows). (d) The transducer is placed in a sagittal plane for a short view of the tendon.

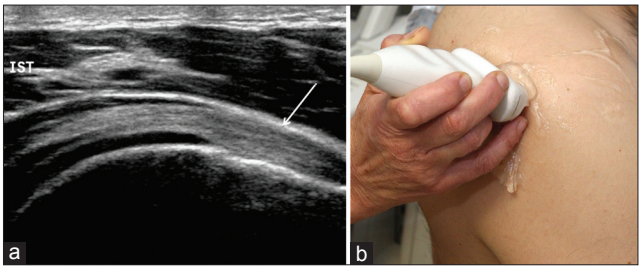

Figure 3: Infraspinatous and teres minor tendons. (a) The infraspinatous tendon (arrow) is seen lying superficial to the echogenic cortical bone of the humeral head and deep to the echogenic bursal fat stripe. (b) The position of the transducer in an axial plane over the infraspinatus fossa.

maneuvers. The transducer is placed over the acromion. Patient's arm is abducted with the elbow flexed to 90°, or/ and the arm is extended anteriorly [Figure 5]. Finally, the acromioclavicular joint is scanned. Patients hand is placed palm up on the thigh. The transducer is positioned over the shoulder top in a coronal plane [Figure 6].

Tendons are seen as a fine fibrillar echogenic structure. Examiners must be aware of anisotropy- a common artifact and potential pitfall in US of tendons, making them appear hypoechoic when the incident ultrasound beam angle is not perpendicular to the tendon. This phenomenon can be avoided by ensuring that the transducer is correctly positioned.[5-6]

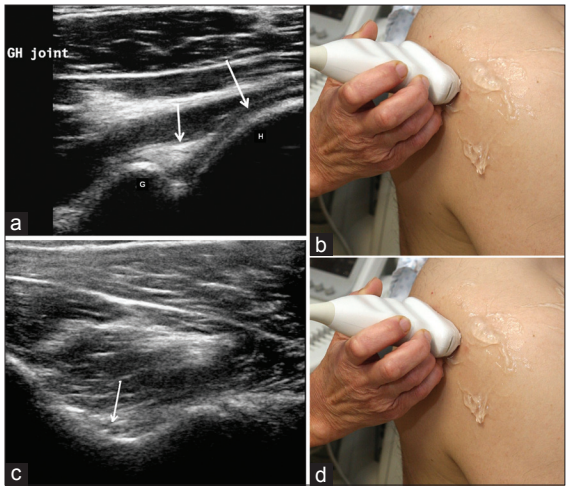

Figure 4: Glenohumeral joint and spinoglenoid notch. (a) Glenohumeral joint. The image shows the humeral head (H) covered by the thin hypoechogenic articular cartilage (long arrow), the glenoid margin (G) and a homogeneously echogenic triangular structure- the fibrocartilagenous posterior labrum (short arrow). (b) The transducer is positioned slightly lower and medially in an axial plane. (c) Spinoglenoid notch. The image shows the suprascapular nerve together with the artery and vein running in this notch (arrow). (d) The transducer is moved slightly medially to view the spinoglenoid notch.

Rotator cuff pathologies

Rotator cuff tears are the most common pathology found in shoulder US examinations.[7] The incidence of tears increases with age. Tendon tears may be classified according to the extent of fiber failure, ranging from complete tears [Figure 7], full-thickness tears [Figures 8, 9], partial-thickness tears [Figures 10-12], and intrasubstance tears [Figure 13]. An acute tear is usually accompanied by joint or bursal effusion [Figure 12].[7-9] Absence of effusion is usually related to chronic tears.[9] In a meta-analysis on the accuracy of MRI, MR arthrography, and US in the diagnosis of rotator cuff tears, US offered high sensitivity and specificity for the assessment of full-thickness rotator cuff tears (92.3 and 94.4%, respectively) with 85.1% and 92%, respectively for all tears.[7] Partial thickness tear appears as a hypoechoic defect or cleft in the tendon, affecting only part of its thickness, while a full-thickness tear extends from the bursal to the articular surface of the tendon. A complete tear is a full-thickness tear affecting the full width of the tendon. The tendon retracts medially, the amount of retraction depending on the age of the tear. In chronic ruptures, the tendon dissapears beneath the coracoacromial arch, leaving the humeral head uncovered by the supraspinatous, the so-called "naked head" sign.

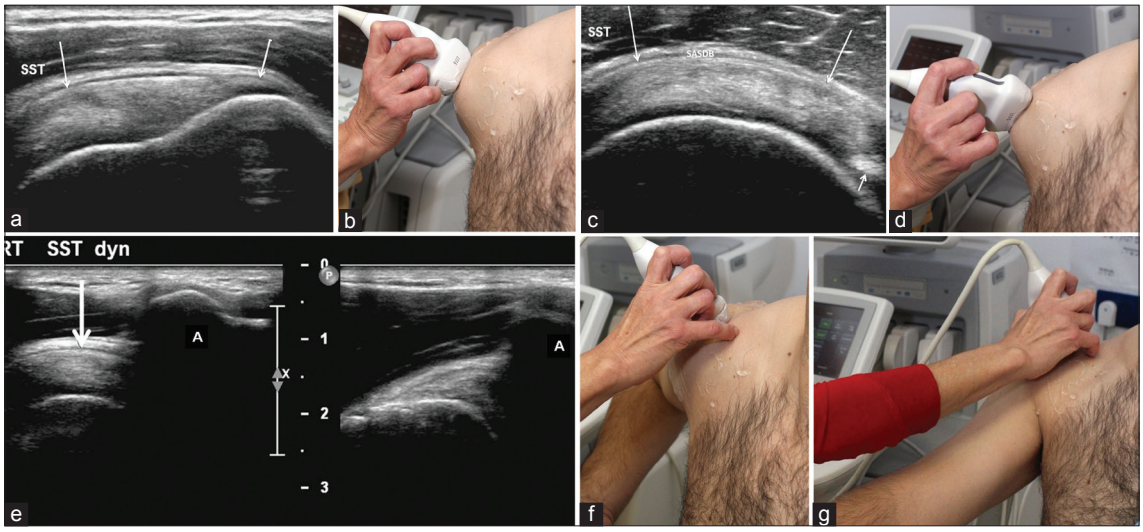

Figure 5: Supraspinatous tendon and dynamic maneuvers. (a) Long axis view of the supraspinatous tendon. The tendon has a homogeneous pattern of medium-level echoes and a convex beak-like shape. From superficial to deep, note the echogenic skin and subcutaneous fat, the hypoechogenic deltoid muscle, the echogenic fat stripe, the hypoechogenic fine subacromial-subdeltoid bursa (arrows) and the supraspinatous tendon lying over the hypoechogenic cartilage of the humeral head, the echogenic cortex of the humeral head and the greater tuberosity. (b) Position of the transducer, in a sagittal plane lateral to the bicipital groove. (c) Short axis view of the supraspinatous tendon (long arrows). The tendon lies between the humeral cartilage below and the subacromial subdeltoid bursa above (SASDB). Note the short axis view of the biceps tendon medially to the supraspinatous, appears as an oval echogenic structure (small arrow). (d) Note the position of the transducer in the axial plane. (e) Dynamic scanning. Left plot shows Supraspinatous tendon and subacromial bursa (arrow) lateral to the acromion (A) Right plot: During dynamic maneuvers, the supraspinatous tendon and subacromial bursa are scanned while gliding beneath the subacromial space (A). (f) The transducer is positioned over the acromion while the patient raises his/her arm. (g) The patient extends the arm forward.

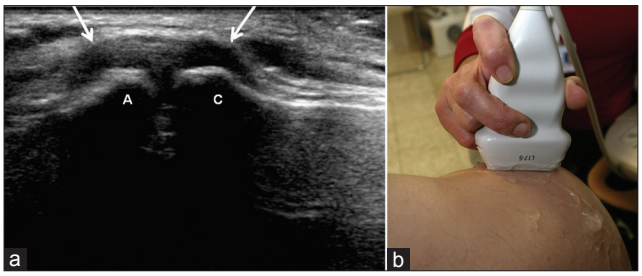

Figure 6: Acromioclavicular joint. (a) The medial edge of the acromium (A), clavicular edge (C) and joint capsule (arrows) are seen. (b) The transducer is positioned in a coronal plane, over the acromion.

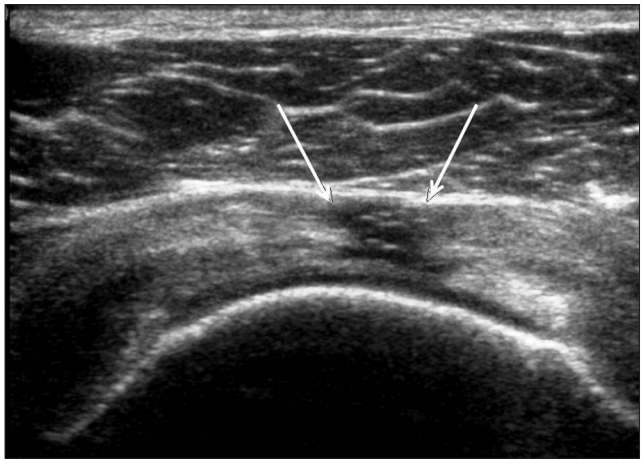

Figure 8: Full-thickness tear. The image shows a sonolucent defect (arrows) extending across the width of the supraspinatous tendon. The tendon is non-retracted and visualized on both sides of the tear.

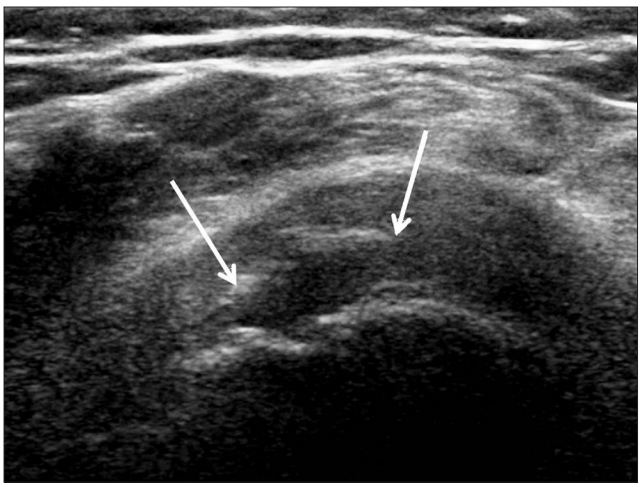

Figure 10: Joint surface partial-thickness tear. The image shows the tear at the articular side of the supraspinatous tendon as a hypoechoic defect with echogenic boundary (arrows). The defect was persistent on all axial and sagital imaging planes.

US findings include nonvisualization of the tendon and herniation of the deltoid muscle. Intrasubstance tears remain localized in the tendon without involvement of its margins. Intrasubstance and partial-thickness tears may be difficult to differentiate from focal tendinopathy.

Figure 7: Complete full thickness tear of the supraspinatous tendon. Tendon nonvisualization in a patient with completely retracted tear (arrows).

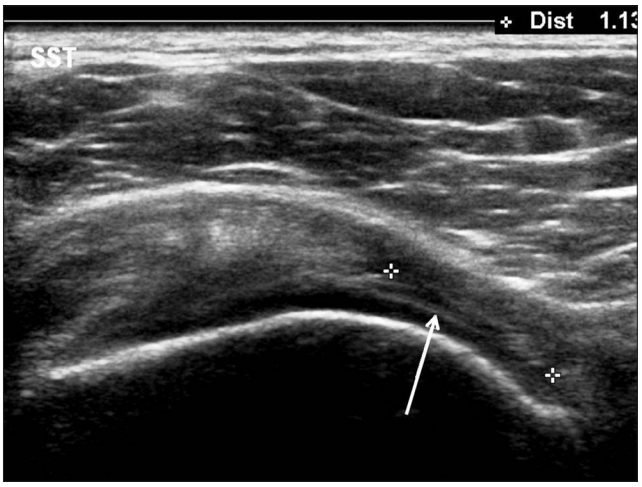

Figure 9: Minimally retracted full-thickness tear. Tear at the greater tuberosity attachment of the supraspinatous tendon, appears as a sonolucent gap (cursors). Note the echogenic line below the tear (arrow) represents the articular cartilage edge, which is well visualized due to fluid in the above tendon tear.

Figure 11: Bursal surface partial-thickness tear. The image shows a sonolucent defect at the bursal side of the supraspinatous tendon (large arrows). Note flattening of the acromio clavicular bursa at the level of the tear (small arrow).

The most commonly found nontear-related pathologies of the rotator cuff are rotator cuff tendinosis [Figure 14], rotator cuff calcifying tendonitis [Figure 15], and subacromial tendon impingement [Figure 16]. It is worthwhile noting that in such cases, tears may develop due to tendon weakness [Table 2].[7,9] Rotator cuff tendinosis or tendinopathy presents as swelling of the tendon with a heterogeneous hypoechoic tendon echotexture. Rotator cuff calcifications appear as hyperechoic foci, either with welldefined posterior shadowing (Type I) or with a faint (Type II) or absent (Type III) shadow. Type I corresponds to the formative phase and Types II and III to the resorptive phase, in which they change to semi or totally liquid deposits of calcium. In subacromial impigment, tendon gliding in the subacromial space during abduction and anterior elevation of the arm is absent.

Figure 12: Bursal surface partial-thickness tear with bursal fluid. The image shows a large sonolucent defect in the bursal side of the supraspinatous tendon (cursors). Fluid in the subscapularis subdeltoid bursa is seen, secondary to an acute tear (arrow).

Figure 14: Rotator cuff tendinosis. The image reveals supraspinatous tendon degeneration as tendon widening with internal echostructure heterogeneity (arrow).

Non-rotator cuff pathologies

Gleno-humeral joint effusion [Figure 17], subacromial-subdeltoid bursa effusion [Figure 18], calcifying bursitis [Figure 19], acromio-clavicular joint arthropathies and dislocation [Figure 20], biceps tendon tear [Figure 21], synovitis [Figure 22], and dislocation [Figure 23] are the main nonrotator cuff-related pathologies seen in shoulder US [Table 3].[8-9] US is sensitive for the detection of glenohumeral joint effusion and subacromial subdeltoid bursal effusion, even in small amounts. Fluid aspiration

Table 2: Rotator cuff pathologies

Rotator cuff tears
Partial-thickness tear
Full-thickness tear
Complete and massive tear
Tendinosis
Calcifying tendinitis
Impingement

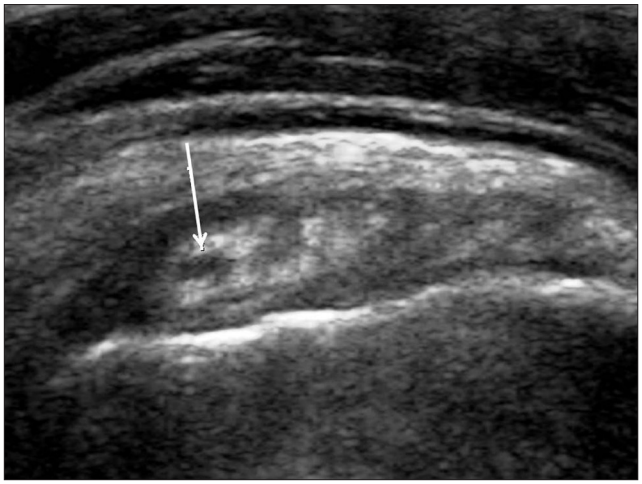

Figure 13: Intrasubstance tear. The short axis image shows central hypoechoic subscapularis tendon defect (arrow).

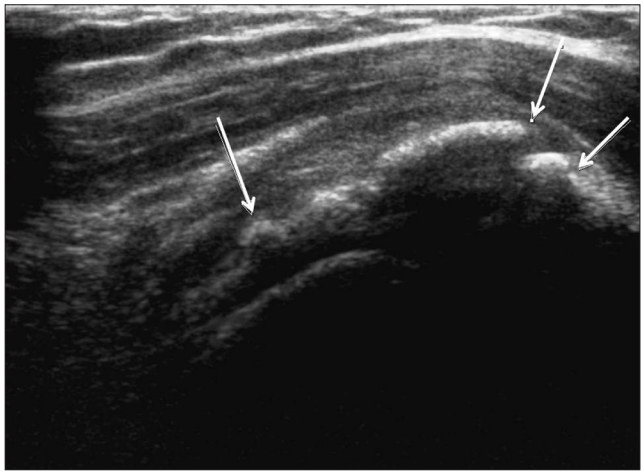

Figure 15: Rotator cuff calcifying tendonitis. Extensive foci of calcifications in the supraspinatous tendon. The image shows calcium deposition as intrasubstance hyperechoic foci with posterior acoustic shadowing (arrows) Type I calcific tendonitis.[9]

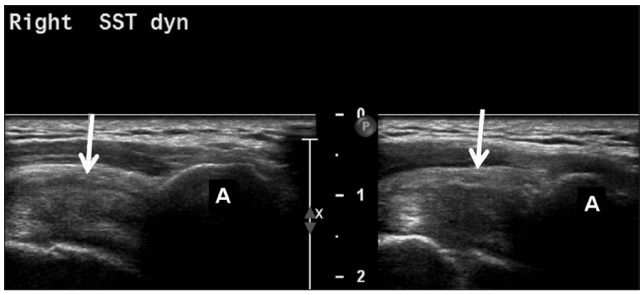

Figure 16: Subacromial tendon impingement. Split image shows the acromion (A) and supraspinatous tendon (arrow). Right plot: the shoulder is in a resting position. Left plot: the patient abducts the shoulder while the arm is in internal rotation. The supraspinatous tendon is seen bunching up lateral to the acromion.

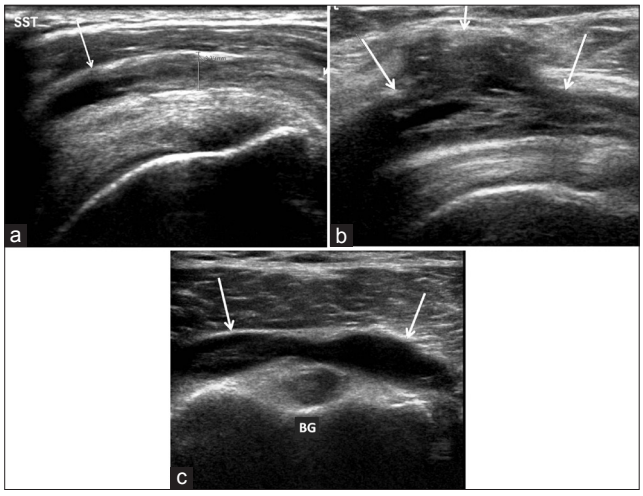

Figure 18: Subacromial-subdeltoid bursal effusion. (a) Septic bursitis. The subacromial-subdeltoid bursa is distended (cursors) and filled with fluid and echogenic material (arrows), (b) Bursal hematoma. Mixed sonolucent and echogenic material filling the bursa in a patient after acromioplasty, (c) Clear bursa synovial fluid. The axial image shows sonolucent fluid in the bursa, over the bicipital tendon in the bicipital groove. Note hypoechogenicity of the biceps tendon in axial scan due to anisotropy.

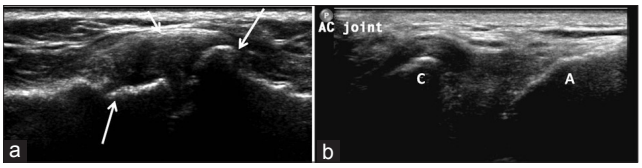

Figure 20: Acromio-clavicular joint pathology. (a) Acromio-clavicular joint arthropathy and subluxation. Transverse scan over the right acromio-clavicular joint shows slight widening of the joint space between the acromion (lower long arrow) and the distal end of the clavicle (upper long arrow). Increase in soft tissue width interposed between bone ends of the joint (short arrow) and associated irregularity of the articular surfaces are consistent with subluxation secondary to degenerative arthropathy. (b) Acromio-clavicular joint dislocation. Marked widening of the joint space between lateral end of the clavicle (C) and acromion (A) in a patient with chronic traumatic dislocation of the left acromio-clavicular joint, confirmed by plain films (not shown).

Table 3: Non-rotator cuff pathologies
Gleno-humeral joint effussion
Subacromial-subdeltoid bursa effussion
Calcifying bursitis
Acromio-clavicular joint arthropathies
Biceps tendon tear, synovitis and dislocation

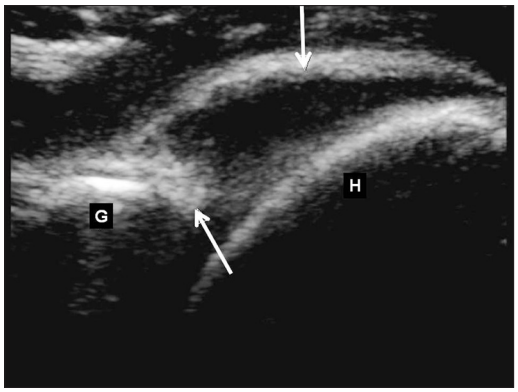

Figure 17: Gleno-humeral joint effusion.The image shows fluid distending the glenohumeral joint capsule (long arrow). Hyperechoic posterior labrum (small arrow) adjacent to the glenoid edge (G) is separated from the humeral head (H) by synovial fluid.

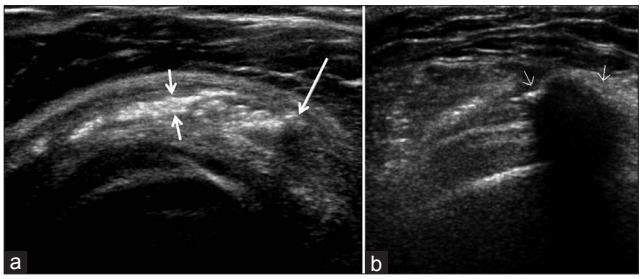

Figure 19: Calcifying bursitis. (a) The image shows hyperechoic material within the subacromial subdeltoid bursa compatible with calcific deposits, most commonly calcium hydroxyapatite crystal, distension of the bursa (small arrows) by the extensive bursal calcification. Few deposits generate acoustic shadowing (large arrow), (b) Wide posterior acoustic shadow in calcific bursitis. The finding was correlated with shoulder radiography (not shown).

Figure 21: Biceps brachii tendon tear. Longitudinal scan of the bicipital groove shows proximal retraction of the biceps muscle (long arrow). A fluid-filled gap with echogenic clots (small arrow) at the myotendinous junction.

under US guidance allows an accurate diagnosis. Intrabursal penetration of calcific deposits in the tendon causes a painful acute microcrystaline bursitis. Subluxation or dislocation of the acromioclavicular joint appears as widening of the joint cavity and bulging of the superior

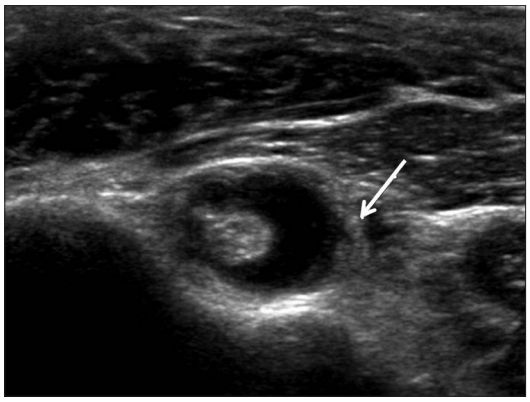

Figure 22: Biceps brachii tendon synovitis. Axial scan of the biceps tendon shows fluid and synovial thickening (arrow) surrounding the biceps tendon sheath.

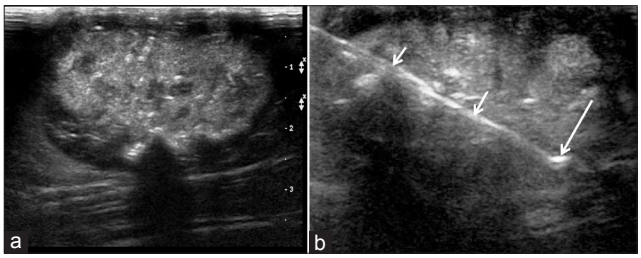

Figure 24: Ultrasound-guided biopsy. (a) Echogenic soft tissue oval mass in the subcutaneous fat at the proximal arm, with multiple foci of calcification (b) Needle biopsy performed with a 16-G tru-cut needle (small arrows) under ultrasound guidance. After firing, the needle tip is seen as a strong echogenic dot (larger arrow). The patient suffered from breast carcinoma and had recently been diagnosed with papillary cystoadenocarcinoma of the ovary. Pathology revealed a metastasis from ovarian carcinoma.

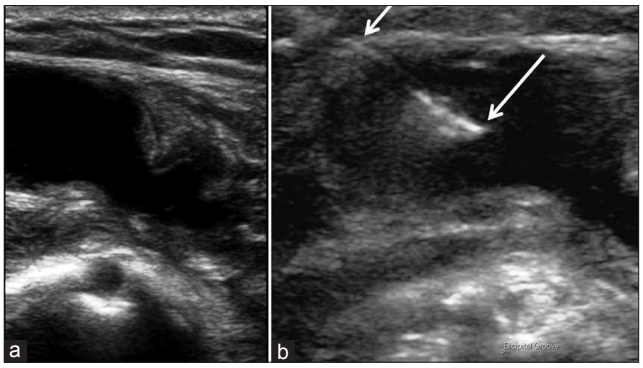

Figure 26: US-guided fluid aspiration. (a) Subacromial-subdeltoid bursa synovitis in a patient with septic arthritis, (b) A 20-G spinal needle is guided into the bursa (arrow) and fluid is aspirated. Bacteriology was positive for *Staphylococcus*.

capsule and ligament. Rupture of the long head of the biceps brachii tendon typically generates a lump in the anterior arm, known as "Popeye sign". Tendon disruption occurs usually at the intrarticular level with distal retraction, leaving an empty groove. In acute tears the tendon stump appears surrounded by fluid. Medial biceps tendon dislocation is diagnosed with US on transverse scans, which depict the bicipital sulcus and the tendon overlying the lesser tuberosity.

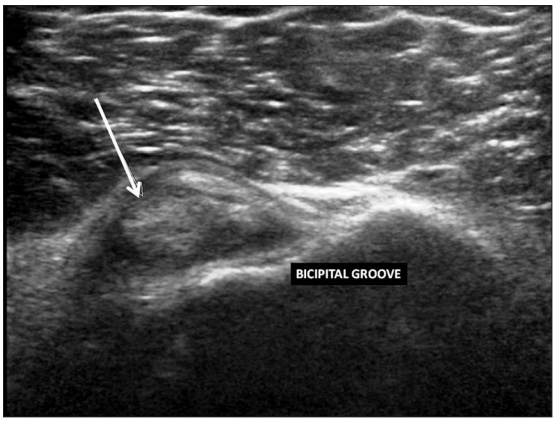

Figure 23: Biceps tendon subluxation. Transverse scan through the left BG shows an empty groove. Note that the groove in this patient is shallow. The biceps tendon (arrow) lies medially, anterior to the lesser tuberosity of the humerus. A small amount of fluid is seen in the tendon sheath.

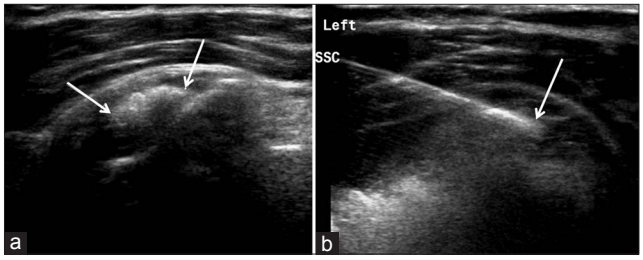

Figure 25: US-guided needle aspiration of calcific deposits in the supraspinatous tendon. (a) Calcific tendonitis, (b) A 20-G spinal needle is directed into the calcific material in the tendon (arrow). Using to and fro movements of the needle, the calcium is indented by the needle. The calcifications can then be removed using needle aspiration.

Shoulder US-guided interventions

Beyond the benefits of US as a diagnostic tool, interventional procedures under US guidance, such as local anesthetic and steroid injection therapy, fluid aspiration in synovial processes, and biopsies of masses, may be accurately performed. US guidance allows precise needle location thus avoiding the risks of intratendinous steroid injection [Figure 24-26].[10]

CONCLUSIONS

Shoulder US has become the modality of choice for the diagnosis of rotator cuff and non-rotator cuff pathologies, offering a high level of diagnostic specificity and sensitivity along with significant benefits to the examiner and the patient, assuming the study is performed by an experienced examiner with high-capacity equipment. US is noninvasive, relatively inexpensive and allows for easy comparison between the affected shoulder and the contralateral side. Strict compliance with procedure protocol, and a comprehensive knowledge of shoulder anatomy, pathologies, and potential technical pitfalls are all needed to make accurate diagnoses. Dynamic imaging and color/

power Doppler US add information unavailable through MRI and arthrography. US guidance adds the benefits of accuracy and safety in interventional procedures such as anesthetic and steroid injections.

REFERENCES

1. Resnick D. Shoulder arthrography. Radiol Clin North Am 1981;19:243- 52.
2. Morag Y, Jacobson JA, Miller B, De Maseener M, Girish G, Jamadar D. MR imaging of rotator cuff injury: What the clinician needs to know. Radiographics 2006;26:1045-65.
3. Erickson SJ. High-resolution imaging of the musculoskeletal system. Radiology 1997;205:593-618.
4. Le Corroller T, Cohen M, Aswad R, Pauly V, Champsaur P. Sonography of the painful shoulder: Role of the operator's experience. Skeletal Radiol 2008;37:979-86.
5. ACR-AIUM Practice guideline for the performance of the musculoskeletal ultrasound examination. Available from: http://www.aium.org/publications/guidelines/musculoskeletal.pdf.
6. Jacobson JA. Shoulder US: Anatomy, technique and scanning pitfalls. Radiology 2011;260:6-16.
7. de Jesus JO, Parker L, Frangos AJ, Nazarian LN. Accuracy of MRI, MR arthrography, and ultrasound in the diagnosis of rotator cuff tears: A meta-analysis. Am J Roentgenology 2009;192:1701-7.
8. Martinoli C, Bianchi S, Prato N, Pugliese F, Zamorani MP, Valle M, et al. US of the Shoulder: Non-rotator cuff disorders. Radiographics 2003;23:381-401.
9. Gaitini D, Militianu D, Nachtigal A, Dogra V. Imaging of the Shoulder. In: Dogra V, Gaitini D, editors. Musculoskeletal ultrasound with MRI correlations. Stuttgart and New York: Thieme Medical Publishers; 2010.p. 1-21.
10. Bianchi S, Zamorani MP. US-guided interventional procedures. In: Bianchi S, Martinoli LE, editors. Berlin Heidelberg: Pringer-Verlag; 2007.

Source of Support: Nil, **Conflict of Interest:** None declared.